

## Chapter II Climate and Meteorology

### Where does precipitation water come from?

#### Introduction

The source of water vapor existing over Mongolia has been considered to consist of evapotranspiration at several regions such as Atlantic Ocean and tropical Asia. During 2003, the intensive observation was conducted in eastern Mongolia. Water samples collected from precipitation, near-surface vapor, and vapor in the free atmosphere were analyzed to investigate the isotopic composition during the warm season. In this study, we develop an isotope transport model, which can estimate the water sources in Mongolia. The simulated water sources were examined with the observations.

#### Model description

A Single-layer multi-tracer transport model is developed into the regional climate model<sup>(1)</sup>. The calculation domain covers 12,000 x 9,000 km range centered on the Tibetan Plateau with 150 km horizontal resolution. The model can reproduce the intraseasonal variation of oxygen stable isotope in precipitation (no Figure). Here, sixteen tracers are defined as in Fig. 1, and concentration of each tracer is determined by the amount of evapotranspiration at each region.

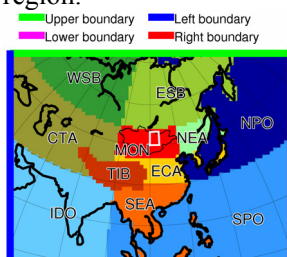


Fig. 1 Definition of regions in the numerical domain of regional climate model. White box shows the area used in Fig. 2.

#### Origin of water vapor

Fig. 2 shows the intraseasonal variation of the water vapor origins over eastern Mongolia. The water vapor in eastern Mongolia is mainly originated by the Central Asia, Siberia, and Mongolia. When the precipitable water (PW) increases as passage of convective systems, water vapor evaporated at Central Asia prominently increases its amount. Thus, synoptic-scale disturbances, like cyclones and front systems, transport huge amount of water vapor from the western regions. On the other hand, water vapor evaporated at low-latitude

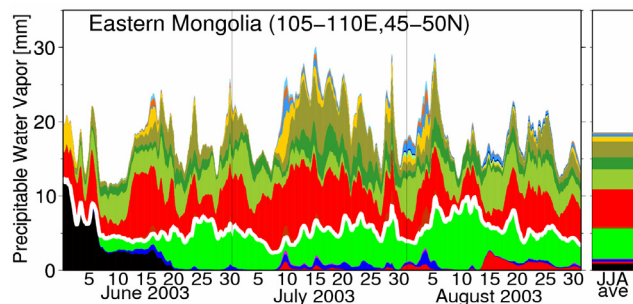


Fig. 2 Time series of water vapor sources over eastern Mongolia as estimated by the multi-tracer model. Colors indicate the amount of evapotranspiration from each region as defined in Fig. 1. Colors below white line are transported through the lateral boundary of the model. Black area indicates the water vapor initially existed in the model domain.

regions contributes very little. The multi-tracer model revealed that the main source of water vapor is not originated at the south but at the west, and most part of water vapor is transported by the synoptic disturbances and ambient westerly during warm season of 2003. However, at Inner Mongolia, more than half portion of the water vapor is coming from low-latitude regions such as Pacific Ocean, Indochina Peninsula, and Indian Ocean during middle

July. Therefore, eastern Mongolia and Northeast China is indeed situated on the margin area between westerly originated moisture and Asian monsoon originated moisture. Even in Mongolia, the contribution of tropical water may increase in the strong monsoon year.

Multi-level isotope observations reveal that the contribution of local evapotranspiration could be 30-46 % near Mongenmorit on 23rd August and 25-44 % at KBU site on 21st August<sup>(2)</sup>. The multi-tracer model estimates approximately 25-40 % of the PW in eastern Mongolia as a local evapotranspiration from 21st through 23rd August.

**References:**

- (1) Sato et al., 2006: Submitted to J. Geophys. Res.
- (2) Tsujimura et al., 2006: J. Hydrol., doi:10.1016 /j.jhydrol.2006.07.025.

**The break in Mongolian rainy season and the relation with the stationary Rossby wave along the Asian jet**

**The break of Mongolian Rainy season**

Seasonal and interannual variation of rainfall over Mongolia was investigated using 10-day rainfall data of 92 stations from 1993 to 2001, and NCEP/NCAR reanalysis data from 1979 to 2001.

Fig. 1 shows the seasonal variation of area-mean rainfall averaged for three different time scales. Mean rainfall increases rapidly from the beginning of June and decreases

rapidly in the middle of August. About 70-80% of the annual precipitation amount occurs from June to August, which is referred to as the "Mongolian rainy season" in this paper. There

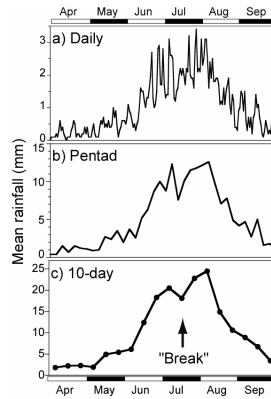


Fig. 1 (Left): Seasonal change of mean daily (a), pentad (b) and 10-day (c) precipitation averaged for 92 stations. The arrow indicates the "break" in the Mongolian rainy season.

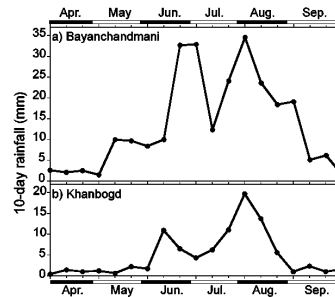


Fig. 2 Time series of mean 10-day rainfall at Bayanchandmani (a: BD) and Khanbogd (b: KB). Averaged period of BD and KB are 8 and 9 years, respectively.

is a local minimum in the middle of July in Fig. 1a to 1c, which is "break" in the Mongolian rainy season.

Fig. 2 shows typical seasonal variation of mean 10-day rainfall at Bayanchandmani(BD) with high annual precipitation in the forest steppe vegetation zone and Khanbogd with low annual precipitation in the desert vegetation zone. Mean 10-day rainfall at BD in Fig. 2a reaches a maximum in the beginning of July, decreases to 1/3 the first maximum value in the middle of July (break), and recovers in the beginning of August. The rainfall at Khanbogd in the desert also has a clear break surrounded by two maxima. The break is unrelated to the difference in annual precipitation.

**Possible mechanism for the break**

Fig. 3 shows the difference of mean Z500 in

the break years and mean Z500 in the non-break years for the middle of July. A wave pattern is predominant from 20°E to 140°E along 45°N, and a weak ridge (R2) exists over Mongolia in the break years. This wave pattern corresponds to the stationary Rossby wave trapped in the Asian jet.

Clear breaks in the rainy season were recognized in 5 years among analysis period of 9 years. In the break period, the stationary Rossby wave trapped in the Asian jet was predominant at 200 hPa, and a barotropic ridge

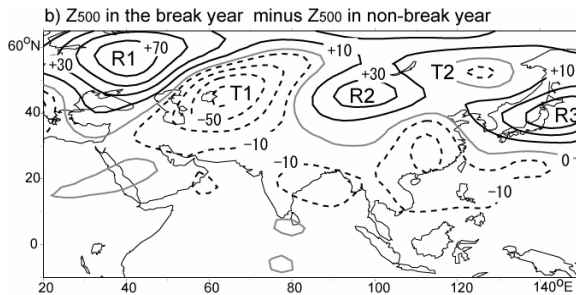


Fig. 3 Difference of 500 hPa height between the break years and non-break years for the middle of July (break years minus non-break years). Contours are every 20 m, but values from -10 m to 10 m are not plotted.

(R2) associated with the Rossby wave developed over Mongolia. Furthermore, interannual variation of the break also corresponded to the variation of the stationary Rossby wave. It is considered that the break of the Mongolian rainy season is caused by the stationary Rossby wave trapped in the Asian jet. The stationary Rossby wave was climatologically phase-locked in seasonal evolution, as a result, the break period was also concentrated around the middle of July.

**References:**

(1) Iwasaki, H., and T. Nii, 2006: The break in Mongolian rainy season and the relation with the stationary Rossby wave along the Asian jet. *J. Climate*, 19, 3394–3405.

# Study on influence of rainfall distribution on NDVI anomaly over the arid regions in Mongolia using an operational weather radar

## Data and analysis region

The relationship between the seasonal distribution of rainfall and the NDVI anomaly are investigated using Ulaanbaator Airport radar data and SPOT NDVI data. Fig. 1 shows the distribution of mean rainfall amount for warm seasons (June to August) from 2003 to 2005 using 1 km CAPPI data. Since data quality along the line N-S is relatively high and there are two vegetation zones (forest steppe and steppe) along it, this line (20 km in width) is adopted to compare the variation of rainfall distribution and NDVI anomaly in view of the vegetation zone.

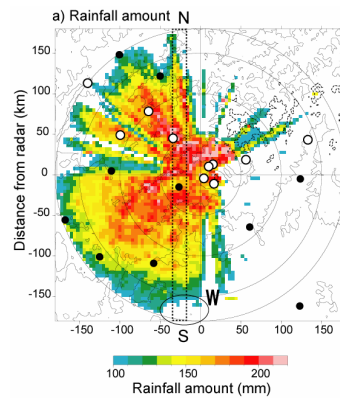


Fig. 1 Distribution of mean rainfall amount for 3 warm seasons using 1 km CAPPI data. The line N-S is a main analysis area. The area denoted by W is a small rainfall area, not a shadow area.

## Influence of rainfall on NDVI anomaly

Fig. 2 shows time-latitude cross sections of 10-day rainfall and NDVI anomaly along the line N-S for 2003 to 2005. As for the steppe vegetation zone (y < +40 km), there are positive NDVI anomalies in July to August of

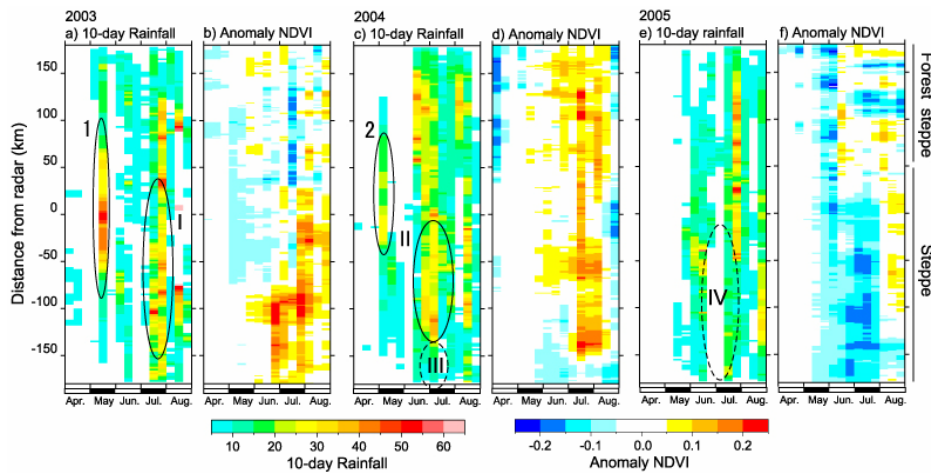


Fig. 2 Time-latitude cross sections of 10-day rainfall and NDVI anomaly along the line N-S for 2003 to 2005. Remarkable rainfall areas (I, II, 1 and 2) and little rainfall areas (III and IV) over the steppe vegetation zone are denoted by ovals.

2003 and 2004 (Figs. 2b and 2d), whereas, the anomaly in July of 2005 (Fig. 2f) is negative. This contrast is predominant among three years. Preceding the positive NDVI anomalies, considerable rainfall is observed in June to July of 2003 and 2004 (I and II in Fig. 2). On the other hand, the negative NDVI anomaly in July is preceded by little rain (IV in Fig. 2). Interannual variation of summer NDVI anomaly corresponds well to radar rainfall amount over the steppe vegetation zone and the time lag is about 10 to 30 days. Thus, weather radar can elucidate that the positive (negative) anomaly of summer NDVI is preceded by a positive (negative) rainfall anomaly. These lag correlation features are consistent with the results of Iwasaki (2006a).

In addition, there is the small area where rainfall amount decreases rapidly around  $y = -140$  km in July of 2004 (III in Fig. 2), in which NDVI anomaly is also negative there; the spatial variation of the NDVI anomaly corresponds well to the rainfall distribution. This low rainfall area was created because mesoscale precipitation systems had passed north of the area. Thus, the weather radar also can monitor the extension of rainfall easily and provide the extension of the positive NDVI anomaly.

#### References:

(1) Iwasaki, H., 2006a: Impact of interannual variability of meteorological parameters on vegetation activity over Mongolia, *J. Meteor.*

*Soc. Japan*, 84, 745-762.

(2) Iwasaki, H., 2006b: Study on Influence of Rainfall Distribution on NDVI Anomaly over the Arid Regions in Mongolia Using an Operational Weather Radar, *SOLA*, 2, 168-171.

## Diurnal variation of convective activity and precipitable water around Ulaanbaator, and impact of soil moisture on convective activity in the nighttime

### Diurnal variation of convective activity around Ulaanbaator

The diurnal variations of convective activity and precipitable water were investigated using an airport radar and GPS receivers around Ulaanbaator (UB), Mongolia; this location was considered as an example of an arid region. The convective activity exhibited a pronounced diurnal cycle (Fig. 1). The convective activity

due to deep convection increased rapidly at 11 LST, reached the maximum at 14 LST, and almost disappeared until 19-20 LST. On the other hand, no diurnal variation of precipitable water could be observed, which implied that there was no considerable evapotranspiration and the diurnal variation of convective activity was irrelevant to the variation of water vapor.

It is noted that the deep convection had almost disappeared until evening, which was a feature different from some humid regions. The reason why cumulonimbus clouds could not develop at night is discussed using numerical modeling from the viewpoint of soil moisture in the next section.

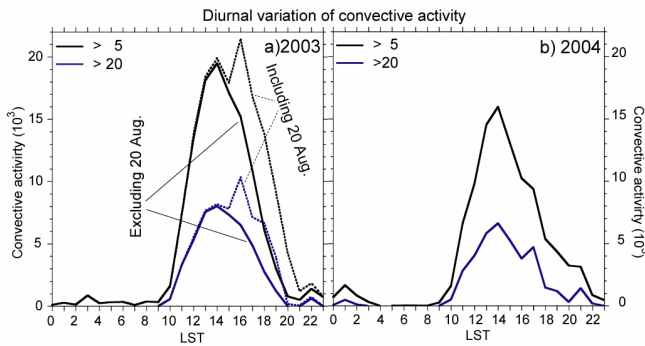


Fig. 1 The diurnal variation of the total rainfall amount over the analysis region using hourly rainfall values greater than 5 mm and 20 mm for 2003 (a) and 2004 (b).

**Impact of soil moisture on convective activity**

Fig. 2 shows the diurnal variation of the 5-day integrated hourly rainfall over the analysis region for each run type (see, Table 1). In the moist soil conditions assumed for humid simulations (SM05 and SM07), an increase in the water vapor in the lower atmosphere due to evapotranspiration led to a potentially unstable condition that was sustained until night. Cumulonimbus clouds were formed at the southern foot of mountains where topographical convergence was expected. On the other hand, in the dry soil conditions assumed for the arid simulations (SM01 and SM03), cumulonimbus clouds did not occur at nighttime even though topographical convergence was expected over the southern foot of the mountains. These features of dry soil conditions were consistent with the results from radar observations around

UB. That is, since the soil around UB is too dry in practice to sustain an unstable condition until night, the deep convection had to decay by night and could not be initiated at night.

Table 1: Run types

Run type	SM01	SM03	SM05	SM07
Soil moisture	0.1	0.3	0.5	0.7

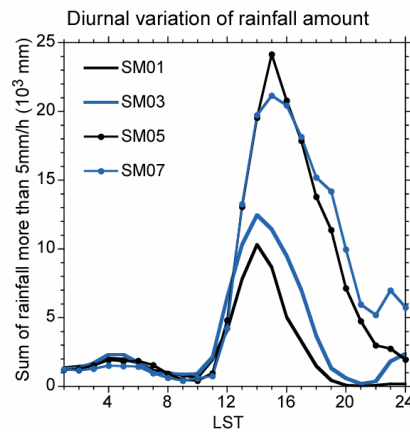


Fig. 2 The diurnal variation of total rainfall amount for SM01 to SM07.

**References:**

(1) Iwasaki, H., T. Sato, T. Nii, F. Kimura, K. Nakagawa, I. Kaihotsu and T. Koike, 2007: Diurnal variation of convective activity and precipitable water around Ulaanbaator, Mongolia, and impact of soil moisture on convective activity in the nighttime. Submitted for Mon. Wea. Rev.